

# Glucocorticoid Receptor Transactivation Is Required for Glucocorticoid-Induced Ocular Hypertension and Glaucoma

Gaurang C. Patel, J. Cameron Millar, and Abbot F. Clark

North Texas Eye Research Institute, University of North Texas Health Science Center, Fort Worth, Texas, United States

Correspondence: Abbot F. Clark, North Texas Eye Research Institute, University of North Texas Health Science Center, 3500 Camp Bowie Boulevard, Fort Worth, TX 76107, USA; [abe.clark@unthsc.edu](mailto:abe.clark@unthsc.edu).

Submitted: December 6, 2018  
Accepted: March 19, 2019

Citation: Patel GC, Millar JC, Clark AF. Glucocorticoid receptor transactivation is required for glucocorticoid-induced ocular hypertension and glaucoma. *Invest Ophthalmol Vis Sci*. 2019;60:1967–1978. <https://doi.org/10.1167/iovs.18-26383>

**PURPOSE.** Glucocorticoid (GC)-induced ocular hypertension (GC-OHT) is a serious side effect of prolonged GC therapy that can lead to glaucoma and permanent vision loss. GCs cause a plethora of changes in the trabecular meshwork (TM), an ocular tissue that regulates intraocular pressure (IOP). GCs act through the glucocorticoid receptor (GR), and the GR regulates transcription both through transactivation and transrepression. Many of the anti-inflammatory properties of GCs are mediated by GR transrepression, while GR transactivation largely accounts for GC metabolic effects and side effects of GC therapy. There is no evidence showing which of the two mechanisms plays a role in GC-OHT.

**METHODS.** GR<sup>dim</sup> transgenic mice (which have active transrepression and impaired transactivation) and wild-type (WT) C57BL/6J mice received weekly periocular dexamethasone acetate (DEX-Ac) injections. IOP, outflow facilities, and biochemical changes to the TM were determined.

**RESULTS.** GR<sup>dim</sup> mice did not develop GC-OHT after continued DEX treatment, while WT mice had significantly increased IOP and decreased outflow facilities. Both TM tissue in eyes of DEX-treated GR<sup>dim</sup> mice and cultured TM cells isolated from GR<sup>dim</sup> mice had reduced or no change in the expression of fibronectin, myocilin, collagen type I, and  $\alpha$ -smooth muscle actin ( $\alpha$ -SMA). GR<sup>dim</sup> mouse TM (MTM) cells also had a significant reduction in DEX-induced cytoskeletal changes, which was clearly seen in WT MTM cells.

**CONCLUSIONS.** We provide the first evidence for the role of GR transactivation in regulating GC-mediated gene expression in the TM and in the development of GC-OHT. This discovery suggests a novel therapeutic approach for treating ocular inflammation without causing GC-OHT and glaucoma.

**Keywords:** glucocorticoid receptor, intraocular pressure, mouse, transactivation, trabecular meshwork

Natural glucocorticoids (GCs) (cortisol in humans and corticosterone in rodents) have received increased attention since their discovery in the early 1950s as a class of steroid hormones released in response to stress. GCs regulate a plethora of functions influencing carbohydrate, lipid and protein metabolism, development, homeostasis, cognition, and inflammation.<sup>1</sup> Exogenous chemically derived GCs (such as dexamethasone [DEX] and prednisolone) are the most widely prescribed medications worldwide because of their broad spectrum of anti-inflammatory and immunomodulatory activities.<sup>2,3</sup> Therapeutic GCs are prescribed to approximately 1.2% of United States<sup>4</sup> and 0.85% of United Kingdom<sup>5</sup> populations, and the estimated worldwide use of GCs is more than \$10 billion per year.<sup>1</sup> GCs remain the mainstay of treatment for clinical management of inflammatory eye diseases including uveitis,<sup>6–8</sup> macular degeneration,<sup>9</sup> optic neuritis, conjunctivitis, and diabetic retinopathy.<sup>10,11</sup> They are also widely used to treat and prevent corneal transplant rejection.<sup>12,13</sup> Unfortunately, long-term use of GCs as therapeutics are limited by serious local and systemic side effects. Higher GC dosages and long-term GC therapy have many ocular side effects including the development of posterior subcapsular cataracts and the development of GC-induced ocular

hypertension (GC-OHT) that can cause iatrogenic open-angle glaucoma and irreversible vision loss.

Early studies have shown an important relationship between GCs and primary open angle glaucoma (POAG). Levels of cortisol have been reported to be elevated in the plasma and aqueous humor of POAG patients,<sup>14–18</sup> and altered cortisol metabolism has been reported in trabecular meshwork (TM) cells obtained from POAG patients.<sup>19,20</sup> There is a varying degree of individual responsiveness to GC therapy; 90% of glaucoma patients are steroid responders as compared to 40% of the general population.<sup>21–25</sup> Patients responsive to GCs (“steroid responders”) develop ocular hypertension with open gonioscopic angles and increased outflow resistance in the TM outflow pathway, similar to that seen in POAG. If elevated IOP persists, it can lead to progressive optic nerve damage, optic disc cupping, and glaucomatous visual field defects. Although GC-OHT is a drug-induced secondary glaucoma, it shares many similar features to POAG. In fact GC-OHT, like POAG, causes defects in the outflow pathway such as physical and mechanical changes in microstructure of TM, leading to increased outflow resistance and elevated IOP.<sup>26,27</sup> These biochemical and morphologic changes that alter TM cellular



structure and function include increased TM cell and nucleus size,<sup>28</sup> cytoskeleton reorganization (forming cross-linked actin networks [CLANs]),<sup>29–35</sup> inhibition of phagocytosis,<sup>34</sup> inhibition of cell proliferation and migration,<sup>35</sup> alteration in cellular junctional complexes,<sup>27</sup> and increased extracellular matrix deposition.<sup>35–39</sup> All these changes further alter TM stiffness<sup>40,41</sup> and impair TM functions, clinically similar to what is observed in POAG patients. Thus, understanding molecular mechanisms of GC action and glucocorticoid receptor (GR) signaling will help us design GCs or similar anti-inflammatory agents with a better benefit-risk ratio, and more effective and safer treatment for patients.

The main actions of GCs are mediated by the glucocorticoid receptor (GR), which is a ligand-activated transcription factor belonging to the nuclear receptor superfamily.<sup>42–44</sup> GR is encoded by the *NR3C1* gene and is expressed in nearly all cells where it directly up- and downregulates thousands of genes distinct to each cell type, governing various key tissue and organismal processes. The GR is composed of three functional domains: an N-terminal transactivation domain (NTD), a central zinc finger DNA-binding domain (DBD), and a C-terminal ligand-binding domain (LBD).<sup>42</sup> Embedded within these domains are regions that confer regulatory activity. The transcription activation function domain (AF1) in the NTD helps activate target genes in ligand-dependent fashion. The two zinc finger motifs in the DBD help in DNA binding to glucocorticoid response elements (GREs), nuclear localization, and GR dimerization. The second transactivation domain (AF2) in the LBD helps ligand-induced activation of GR. The two nuclear localization signals located in DBD-hinge and LBD regions help in nuclear localization of activated GR. In the absence of ligand (i.e., GCs), GR predominantly resides in the cytoplasm as part of a large multiprotein complex that includes chaperone proteins (hsp90, hsp70, and p23)<sup>45</sup> and immunophilins (FKBP51 and FKBP52), maintaining the high-affinity ligand-binding GR conformation.<sup>46</sup> Upon ligand binding, GR sheds its cytoplasmic chaperoning complex and translocates to the nucleus, where it acts as a ligand-dependent transcription factor, transactivating or transrepressing specific gene promoters. During transactivation (TA), the ligand-activated GR homodimerizes and acts as a transcription factor by binding to specific DNA sequences on genes carrying GREs to alter gene expression. In contrast, in transrepression (TR), activated GR monomers bind to other transcription factors (e.g., AP-1, NF- $\kappa$ B) independently of direct DNA contact to block them from activating expression of genes that these transcription factors regulate.<sup>1,28</sup> It has been assumed that the undesirable side effects of GC therapy require GR TA activities, while the anti-inflammatory activities are due to TR mechanisms.<sup>47–49</sup>

These two different GR mechanisms have been a driving force for discovery of novel selective glucocorticoid receptor agonists (SEGRAs) or modulators (SEGRMs). SEGRAs are the compounds that promote TR but do not mediate TA.<sup>47</sup> Based on these observations, clinical enthusiasm for the development and use of SEGRAs has grown in recent years as SEGRAs show many of the anti-inflammatory activities of GCs by inhibiting proinflammatory TFs.<sup>50,51</sup> In recent years, SEGRAs have been investigated for treating eye diseases. CpdA and ZK-216346 are among the first discovered and widely used experimental SEGRAs, which favor GR TR and fail to induce GR TA of reporter genes.<sup>52–56</sup> Mapracorat (previously ZK-245186, and subsequently BOL-303242-X) and ZK209614 have shown anti-inflammatory efficacy in suppressing inflammation and allergic conjunctivitis in rabbit models of dry eye and paracentesis-induced inflammation. They show both antiallergic and anti-inflammatory effects without unwanted IOP elevation (i.e., development of GC-OHT). While evaluating myocilin expression in cultured monkey TM cells by BOL-303242-X compared

with DEX and prednisolone acetate,<sup>57</sup> investigators have found that BOL-303242-X results in reduced myocilin expression (at both mRNA and protein levels) compared with DEX or prednisolone acetate. These results suggest that reduced GR TA may limit effects on the conventional outflow pathway. Stamer and colleagues<sup>58</sup> have evaluated the effect of GW870086X on cultured human TM cells and showed that this SEGRA induces fibronectin (FN) production (although less than DEX and prednisolone acetate) but does not induce myocilin (similar to BOL-303242 study<sup>57</sup>) or affect hydraulic conductivity. This compound is not entirely devoid of TA activity with respect to gene expression regulation. Thus, TM cells exhibit variable responses to these different SEGRAs, compared to traditional GCs. Moreover, which of the GR mechanisms (TA and/or TR) is regulating GC-OHT is also currently unknown. This lack of understanding of precise GR mechanisms responsible for pathophysiology of GC-OHT further hinders development of better benefit-risk ratio of GCs, which is a current and ongoing challenge.

To study these two GR mechanisms, Reichardt and colleagues<sup>59</sup> have successfully developed GR<sup>dim</sup> transgenic mice carrying the point mutation A458T in the GR-DBD. GR TA requires binding of receptor homodimers to specific GREs. The D loop of the second zinc finger in DBD of GR is crucial for GR dimerization (i.e., formation of GR homodimers) and GR binding to its GREs in target genes.<sup>60–62</sup> However, introducing a point mutation in the GR DNA binding domain (e.g., in D loop, A458T, replacing alanine with threonine) changes the GR protein structure and thereby impairs the ability of GR to form dimers and bind to specific GREs, thereby impairing and inhibiting GR TA. Interestingly, in GR<sup>dim</sup> mice GRE-dependent gene transcription diminishes, while the TR function (cross-talk with AP-1 and NF- $\kappa$ B) of GR still remains intact.<sup>59,63–65</sup> Following development of GR<sup>dim</sup> transgenic mice, these mice became an important research tool to dissect different GR functions. GR<sup>dim</sup> mice remain viable and appear normal<sup>59</sup> after birth.

In our current study, we used GR<sup>dim</sup> mice to better understand mechanisms responsible for GC-OHT and steroid responsiveness. This will help dissect mechanisms responsible for GC-OHT. We tested the hypothesis that GR TA mediates the GC-induced biochemical and morphologic changes in the TM and contributes to GC-OHT. We used our newly developed mouse model of DEX-induced OHT<sup>66,67</sup> to compare DEX-induced responses between GR<sup>dim</sup> mice and wild-type (WT) mice. This reproducible model is easy to run and captures many aspects of GC-OHT observed in humans, including elevated IOP, reduction in the aqueous humor outflow facility, and biochemical changes in TM.<sup>66,67</sup>

## MATERIALS AND METHODS

### Animals

GR<sup>dim</sup> transgenic mice (on the C57BL/6 background) were acquired from Günther Schütz at Helmholtz Zentrum München, Germany. Animals were bred, and our colony was maintained at University of North Texas Health Science Center. Six- to 8-month-old male and female GR<sup>dim</sup> and WT mice were used for all the experiments. All mouse studies and care were performed in compliance with the ARVO Statement for the Use of Animals in Ophthalmic and Vision Research and the University of North Texas Health Science Center Institutional Animal Care and Use Committee regulations. All experimental protocols were approved by University of North Texas Health Science Center Institutional Animal Care and Use Committee regulations. Mice were housed under controlled conditions of

temperature (21°C–26°C), humidity (40%–70%), and a 12-hour light/12-hour dark cycle. Food and water were provided ad libitum. The number of animals used in each experiment is indicated in the corresponding figure legends and Results section.

### Genotyping of GR<sup>dim</sup> Mice

All the animals were genotyped before experimental use as previously described.<sup>59</sup> Genotyping was performed on DNA isolated (catalog No. 740952.250, Nucleospin tissue kit; Manufacturer, City, State, Country) from ear punches by using specific PCR primers designed to recognize the point mutation on exon 4 of the mouse GR. The PCR reactions were carried out for 35 cycles (94°C, 1 minute; 58°C, 1 minute; 72°C, 1 minute) by using the *Taq* PCR Master Mix Kit (catalog No. 201443; Qiagen, Germantown, PA, USA). The 0.24-kb PCR amplicon was digested with restriction endonuclease *BsrGI* (*Bsp*1407I, catalog No. ER0932; Thermo Fisher Scientific, Inc., Rockford, IL, USA) at 37°C for 16 hours and the products were electrophoresed on 2% agarose gels. The GR<sup>dim</sup> allele will generate a 0.12-kb fragment owing to the introduction of a new restriction site by the point mutation. The following primers were used for genotyping: forward primer (5'-GTGCTTGATGATAGTCTGCTC-3') and reverse primer (5'-CCATTACCTCCAGGTTTCATTC-3').

### Dexamethasone Acetate Formulation and Periocular Conjunctival Fornix Injection

Dexamethasone acetate (DEX-Ac) 10 mg/mL and vehicle suspension were formulated as previously described.<sup>66,67</sup> To develop DEX-Ac-induced OHT in mice, the DEX-Ac suspension was periocularly injected bilaterally by using our previously described procedure.<sup>66,67</sup> Before and during injections, mice were anesthetized with isoflurane (2.5%) containing oxygen (0.8 L/min). For topical anesthesia, both eyes received one to two drops of 0.5% proparacaine HCl (Akorn, Inc., Lake Forest, IL, USA). The lower eyelid was retracted, and the 32-gauge needle with a Hamilton glass microsyringe (25- $\mu$ L volume) (Hamilton Company, Reno, NV, USA) was inserted through the conjunctival fornix (CF). DEX-Ac suspension or vehicle (20  $\mu$ L) was injected immediately into the CF over the course of 10 to 15 seconds. The needle was then withdrawn. The procedure was performed on both eyes of each animal. Mice were treated with DEX-Ac or vehicle once per week until the end of the study.

### IOP Measurements

For this study, IOPs of isoflurane-anesthetized mice were measured twice a week during night. Mice were kept in the dark starting at 4 PM on the day of IOP measurement. At 10 PM the IOPs of anesthetized mice were measured in both eyes by using a TonoLab rebound tonometer as previously described.<sup>66,67</sup> The entire procedure was performed in a darkroom using dim red light.

### Aqueous Humor Outflow Facility Measurements

Aqueous humor outflow facility (C) was measured by using our constant flow infusion technique in live mice as previously described.<sup>66-69</sup> Mice were anesthetized by using a 100/10 mg/kg ketamine/xylazine cocktail. A quarter to half of this dose was administered for maintenance of anesthesia as necessary. One to two drops of proparacaine HCl (0.5%) (Akorn, Inc.) were applied topically to both eyes for corneal anesthesia. The anterior chambers of both eyes were cannulated by using a 30-

gauge needle inserted through the cornea 1 to 2 mm anteriorly to the limbus and pushed across the anterior chamber to a point in the chamber angle opposite to the point of cannulation, taking care not to touch the iris, anterior lens capsule epithelium, or corneal endothelium. Each cannulating needle was connected to a previously calibrated (sphygmomanometer, Diagnostix 700; American Diagnostic Corporation, Hauppauge, NY, USA) flow-through BLPR-2 pressure transducer (World Precision Instruments [WPI], Sarasota, FL, USA) for continuous determination of pressure within the perfusion system. A drop of phosphate-buffered saline (PBS) was also administered to each eye to prevent corneal drying. The opposing ends of the pressure transducer were connected via further tubing to a 50- $\mu$ L syringe loaded into a microdialysis infusion pump (SP101I Syringe Pump; WPI). The tubing, transducer, and syringe were all filled with sterile PBS solution (filtered through a 0.2- $\mu$ m HT Tuffryn Membrane Acrodisc Syringe Filter; PALL Gelman Laboratory, Port Washington, NY, USA). Signals from each pressure transducer were passed via a TBM4M Bridge Amplifier (WPI) and a Lab-Trax Analog-to-Digital Converter (WPI) to a computer for display on a virtual chart recorder (LabScribe2 software; WPI). Eyes were initially infused at a flow rate of 0.1  $\mu$ L/min. When pressures stabilized within 10 to 30 minutes, pressure measurements were recorded over a 10-minute period, and then flow rates were increased sequentially to 0.2, 0.3, 0.4, and 0.5  $\mu$ L/min. Three stabilized pressures at 5-minute intervals at each flow rate were recorded. C in each eye of each animal was calculated as the reciprocal of the slope of a plot of mean stabilized pressure as ordinate against flow rate as abscissa.

### Intracameral Injection of Magnetic Beads

For intracameral injection, a 33-gauge needle with a glass microsyringe (10- $\mu$ L volume) (Hamilton Company) was used. Before and during injection, mice were anesthetized with isoflurane (2.5%) containing oxygen (0.8 L/min). For topical anesthesia, both eyes received one to two drops of 0.5% proparacaine HCl (Akorn, Inc.). Each eye was proptosed and the needle was inserted through the cornea just above the limbal region and inserted into the anterior chamber at an angle parallel to the cornea, taking care to avoid touching the iris, anterior lens capsule epithelium, or corneal endothelium. Up to 2  $\mu$ L 1% (wt/vol) sterile magnetic polystyrene smooth surface beads (2.0–2.9  $\mu$ m in diameter; Spherotech, Inc., Lake Forest, IL, USA) were injected slowly (over a 30-second period). The needle was then withdrawn. The procedure was performed on both eyes of each animal.

### Mouse TM (MTM) Cell Culture and DEX Treatment

MTM cells were isolated from 2- to 3-month-old GR<sup>dim</sup> and WT mice previously injected with magnetic beads, and characterized by using previously developed methodology.<sup>70</sup> MTM cells were cultured and maintained in Dulbecco's modified Eagle's medium-high glucose (Invitrogen-Gibco Life Technologies, Grand Island, NY, USA) supplemented with 10% fetal bovine serum (Atlas Biologicals, Fort Collins, CO, USA), penicillin (100 units/mL), streptomycin (0.1 mg/mL), and L-glutamine (0.292 mg/mL) (Thermo Fisher Scientific). MTM cells from GR<sup>dim</sup> and WT mice were cultured on six-well plates until confluent and then treated with vehicle control (0.1% ethanol) or DEX (100 nM) for another 72 hours.

### Immunocytochemistry

Cells were cultured on glass coverslips in 24-well plates. At the end of the experiment, cells were fixed in 4% paraformalde-

hyde (Electron Microscopy Sciences, Hatfield, PA, USA) and kept at 4°C for 30 minutes. After PBS washing, cells were incubated with 0.5% Triton X-100 (Fisher Scientific, Pittsburgh, PA, USA) in PBS at room temperature for 15 minutes, and then blocked with PBS Superblock (Thermo Fisher Scientific). Cells were then immunolabelled with primary antibodies: rabbit polyclonal FN antibody (1:200, catalog No. AB1945; EMD Millipore, Billerica, MA, USA) or rabbit polyclonal collagen I antibody (1:200, catalog No. NB600-408; Novus Biologicals, Centennial, CO, USA) and incubated at 4°C overnight. Cells incubated without primary antibody served as a negative control. Following the incubation, cells were washed three times with PBS and further incubated for 1.5 hours at room temperature with the secondary antibodies (1:500, Alexa goat anti-rabbit 488; Thermo Fisher Scientific). After PBS washing, glass coverslips with cells were then mounted on ProLong gold anti-fade reagent with DAPI (Invitrogen-Molecular Probes, Carlsbad, CA, USA). All images were taken with a Keyence all-in-one fluorescence microscope (Itasca, IL, USA). All antibodies used in this study have been validated and characterized previously.<sup>66,71</sup>

### Detection and Evaluation of CLANs

MTM cells from GR<sup>dim</sup> and WT mice were cultured on glass coverslips in 24-well plates until confluent. Once confluent, they were treated with vehicle control (0.1% ethanol) or DEX (100 nM) for 7 days. At the end of the experiment, cells were processed as described in Immunocytochemistry until the blocking step. F-actin was stained with phalloidin conjugated with Alexa-488 (1:300; Life Technologies, Eugene, OR, USA) at 4°C overnight. After PBS washes, coverslips were mounted on ProLong gold anti-fade reagent with DAPI (Invitrogen-Molecular Probes). CLANs were visualized by using Nikon Eclipse Ti-U microscope with a Nuance imaging system (Nikon, Melville, NY, USA). CLANs were defined as F-actin-containing cytoskeletal structures with at least one triangular actin arrangement consisting of actin spokes and at least three identifiable hubs.<sup>72</sup> Each coverslip was assessed at nine locations with approximately 80 to 170 cells evaluated per coverslip. Two to three coverslips were evaluated per treatment group. CLAN-positive cells (CPCs), defined as any cell containing at least one CLAN or multiple CLANs, were calculated as the percentage of CPCs by dividing the number of CPCs by the number of DAPI-positive cells.

### Immunohistochemistry

Eyes from DEX-Ac- and vehicle-treated mice were enucleated and fixed overnight in freshly prepared 4% paraformaldehyde in PBS. Afterwards, eyes were washed three times with PBS, dehydrated with ethanol, and embedded in paraffin. Samples were sectioned at 5 µm. For immunostaining, tissue sections were deparaffinized in xylene and rehydrated twice each with 100%, 95%, 70%, and 50% ethanol for 5 minutes. Tissue sections were blocked (10% goat serum + 0.2% Triton X-100) for 2 hours in a dark and humid chamber. Tissue sections were then washed briefly with PBS and immunolabeled with either mouse monoclonal FN antibody (1:200, catalog No. sc18825; Santa Cruz Biotechnology, Dallas, TX, USA), rabbit polyclonal collagen I antibody (1:200, catalog No. NB600-408; Novus Biologicals), or rabbit polyclonal  $\alpha$ -smooth muscle actin ( $\alpha$ -SMA) antibody (1:100, catalog No. ab5694; Abcam, Cambridge, UK) and incubated overnight at 4°C. Tissue sections incubated without primary antibody served as a negative control. Following the incubation, tissue sections were washed three times with PBS and further incubated for 1.5 hours at room temperature with the appropriate secondary antibodies (1:500, Alexa goat anti-

rabbit 488/568 or Alexa goat anti-mouse 488; Thermo Fisher Scientific). Tissue sections were washed with PBS and then mounted on ProLong gold anti-fade reagent with DAPI (Invitrogen-Molecular Probes). Images were captured by Keyence all-in-one fluorescence microscope (Itasca). All antibodies used in this study were validated and characterized previously.<sup>66,71</sup>

### Western Blot Analysis

After DEX treatment, whole cell lysates were collected from GR<sup>dim</sup> and WT MTM cells by using lysis buffer (M-PER; Thermo Fisher Scientific) containing Halt protease inhibitor cocktail (1:100; Thermo Fisher Scientific). After protein estimation using the DC protein assay kit (Bio-Rad, Hercules, CA, USA), 32 µg total protein was used for SDS-PAGE. The protein samples were run on denaturing 12% polyacrylamide gels and transferred onto polyvinylidene difluoride (PVDF) membranes. Blots were blocked with 10% nonfat dried milk for 1 hour and then incubated overnight with specific primary antibodies at 4°C on a rotating shaker. The membranes were washed thrice with 1X phosphate buffered saline/Tween (PBST) and incubated with corresponding horseradish peroxidase (HRP)-conjugated secondary antibody for 1.5 hours. The proteins were then visualized by using enhanced chemiluminescence detection reagents (SuperSignal West Femto Maximum Sensitivity Substrate; Pierce Biotechnology, Rockford, IL, USA). The primary antibodies used were mouse monoclonal FN antibody (1:1000, catalog No. sc18825; Santa Cruz Biotechnology), mouse monoclonal myocilin antibody (1:1000, catalog No. H00004653-M01; Abnova, Taipei City, Taiwan), and glyceraldehyde-3-phosphate dehydrogenase (1:5000, catalog No. 3683; Cell Signaling Technology, Danvers, MA, USA). All antibodies used in this study have been validated and characterized previously.<sup>66,71</sup>

### Statistics

Statistical analyses were performed by using GraphPad Prism Version 7.0 (GraphPad Software, La Jolla, CA, USA). Unpaired Student's *t*-test (2-tailed) was used to compare data between two groups. A *P* < 0.05 was considered statistically significant.

## RESULTS

### Characterization of Isolated GR<sup>dim</sup> and WT MTM Cells

TM cells are actively phagocytic in vitro and in vivo to clear debris and pigment granules in the aqueous humor.<sup>73-76</sup> We took advantage of this activity of TM cells to isolate the MTM cells from GR<sup>dim</sup> and WT mice. We injected magnetic beads into the anterior chamber as described previously.<sup>70</sup> The beads were phagocytized by MTM cells, and then MTM cells with engulfed magnetic beads from tissue digests were separated from non-TM cells by applying a magnetic field. Once in culture, a number of criteria were used to characterize these as TM cells, including the expression of collagen IV (Col IV), laminin,  $\alpha$ -SMA (Figs. 1A, 1B), DEX-induced increase in FN, myocilin, and collagen I expression (Fig. 2), as well as DEX-induced formation of CLANs (Fig. 3).<sup>70</sup> We also confirmed the genotypes of MTM cells isolated from GR<sup>dim</sup> and WT mice (Fig. 1C).

### Biochemical Changes in WT and GR<sup>dim</sup> MTM Cells Upon DEX Treatment

DEX treatment leads to many biochemical changes in the TM cells, including increased production of FN,<sup>36</sup> collagens,<sup>38</sup> and

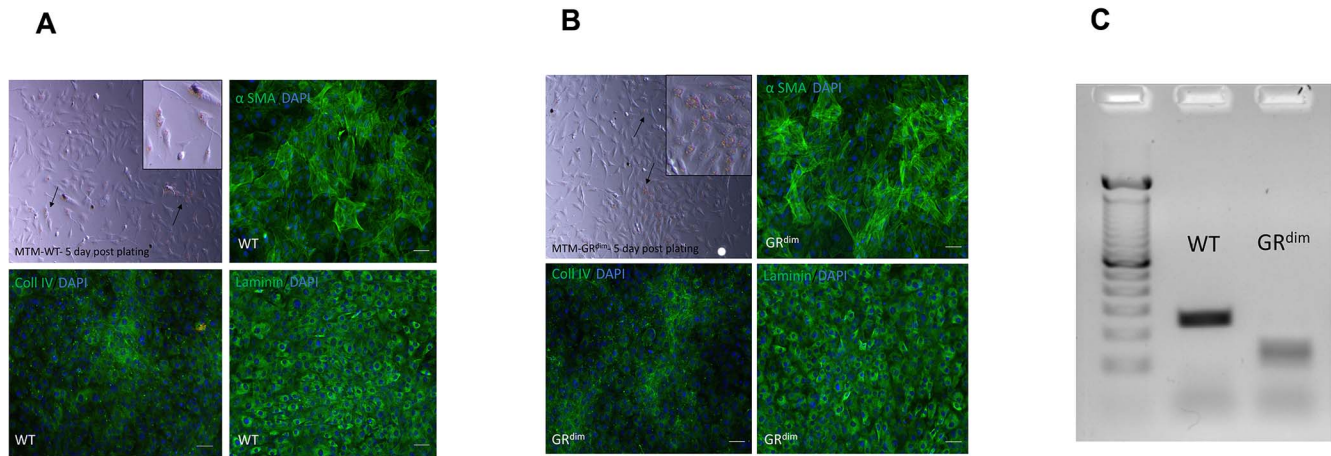


**FIGURE 1.** Characterization of MTM cells from WT (A) and GR<sup>dim</sup> (B) mice. Bright field image showing MTM cells in culture after 5 days of isolation (top left column). Insets are magnified images showing MTM cells with engulfed magnetic beads. The expression of collagen IV (Coll IV) (green) (bottom left column),  $\alpha$ -SMA (green) (top right column), and laminin (green) (bottom right column) in MTM cells from GR<sup>dim</sup> and WT mice is shown by immunocytochemistry. (C) Genotypes of MTM cells from GR<sup>dim</sup> and WT mice. The WT MTM cells show 0.24-kb amplicon, whereas GR<sup>dim</sup> MTM cells show only 0.12-kb fragments owing to the introduction of a new restriction site by the point mutation. Black arrows indicate MTM cells with magnetic beads. Blue color represents DAPI staining showing cell nuclei. Magnification:  $\times 20$ . Representative data for three experimental triplicates (A, B). Scale bar: 50  $\mu$ m.

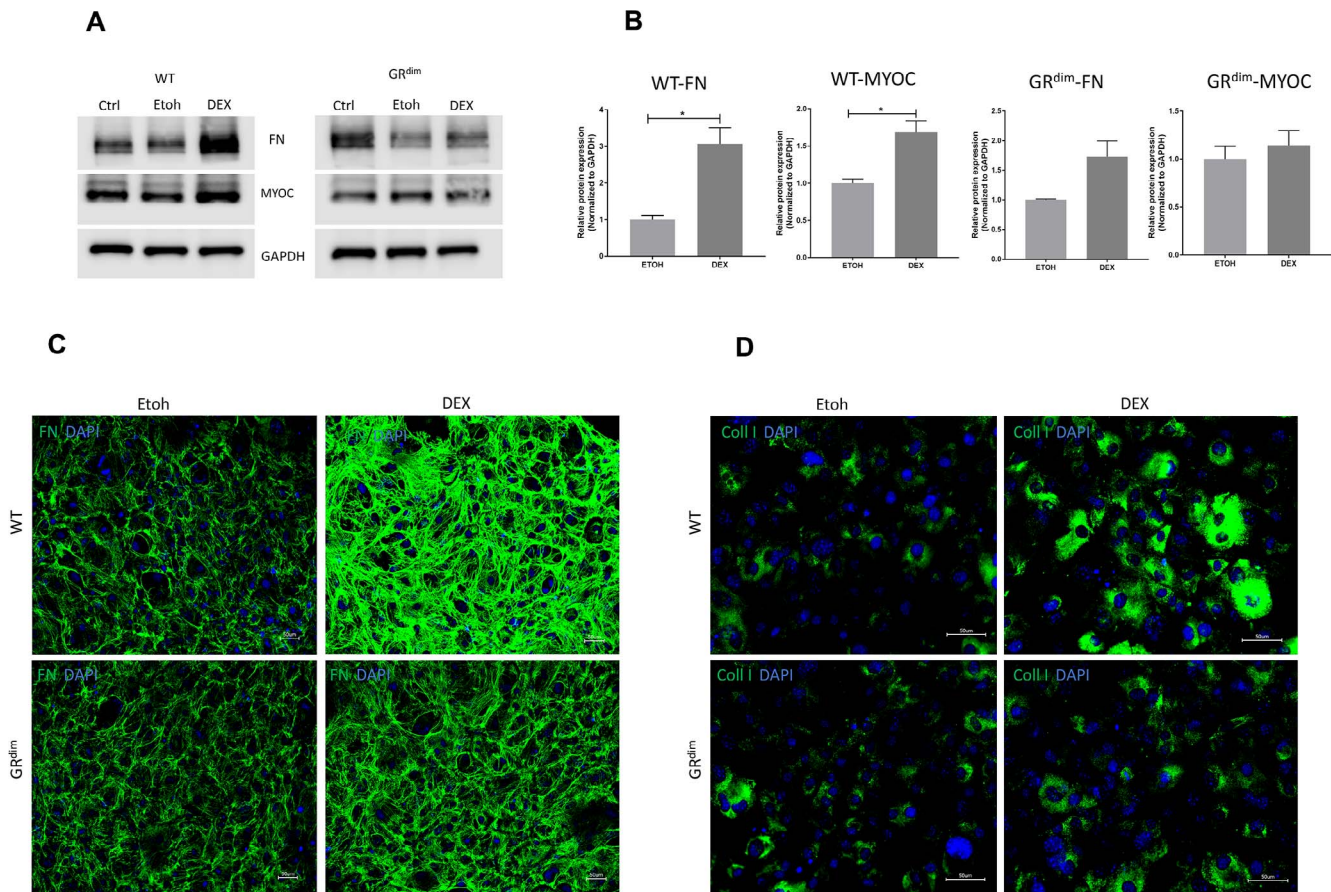


**FIGURE 2.** Inhibition of DEX-induced biochemical changes in GR<sup>dim</sup> MTM cells. (A) Representative Western blot images of FN and MYOC from WT (left) and GR<sup>dim</sup> (right) MTM cells. DEX treatment did not induce expression of FN and MYOC in GR<sup>dim</sup> MTM cells (right), compared to DEX induction in WT MTM cells (left). (B) Quantification of Western blot showing significant increase in FN and MYOC in WT MTM cells compared to GR<sup>dim</sup> MTM cells,  $*P < 0.05$ . Unpaired Student's *t*-test. Data are presented as mean  $\pm$  SEM. Immunostaining of vehicle control and DEX-treated MTM cells showing little FN (green) (C) and collagen I (green) (D) induction upon DEX treatment in GR<sup>dim</sup> MTM cells, while there was clear induction in WT MTM cells. Blue color represents DAPI staining showing cell nuclei. Magnifications:  $\times 20$  (B) and  $\times 40$  (C). Actin served as loading control in (A). Representative data for three experimental triplicates. Scale bars: 50  $\mu$ m. Ctrl, control untreated; Etoh, vehicle (0.1% ethanol) control; MYOC, myocilin.

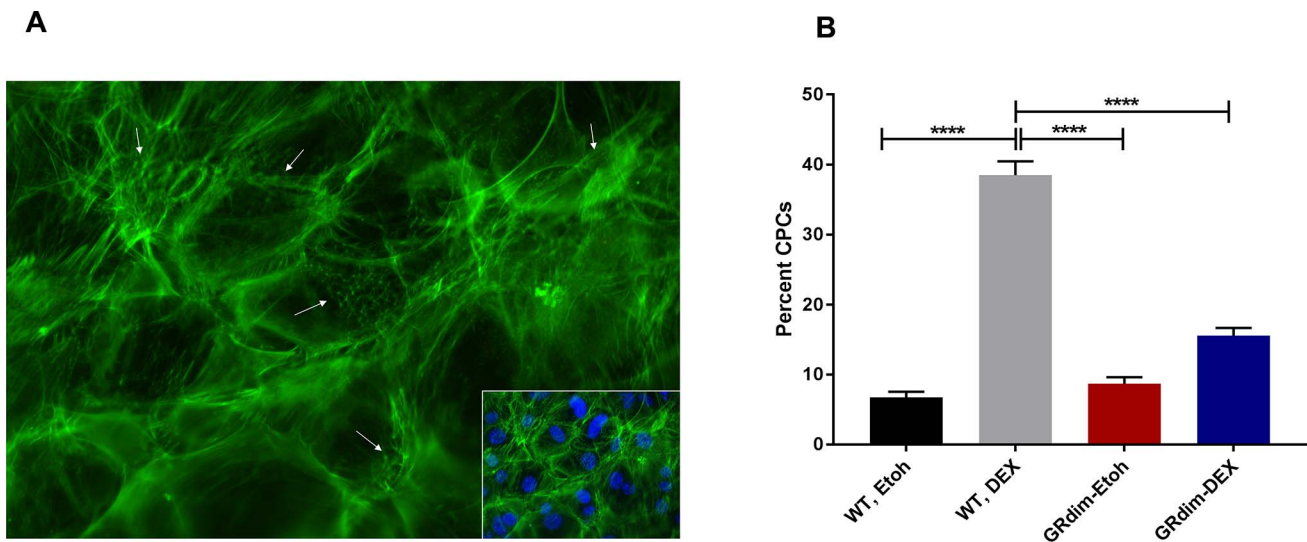


**FIGURE 3.** Formation of DEX-induced CLANs in WT and GR<sup>dim</sup> MTM cells. (A) Representative image of multiple CLANs in WT MTM cells. CLANs were defined as F-actin-containing cytoskeletal structures with at least one triangulated actin arrangement consisting of actin spokes and at least three identifiable hubs. Arrows point to CLANs. Magnification:  $\times 60$ . Inset represents DAPI-merged image. (B) Percentage of CPCs was calculated by dividing the number of CPCs by the number of DAPI-positive cells. CLAN formation was reduced in GR<sup>dim</sup> MTM cells compared with WT MTM cells upon DEX treatment. \*\*\*\* $P < 0.0001$ , 1-way ANOVA. Data are presented as mean  $\pm$  SEM.

myocilin.<sup>77</sup> To compare these DEX-induced biochemical changes between GR<sup>dim</sup> and WT MTM cells, we performed Western immunoblot analysis for FN and myocilin (Figs. 2A, 2B) and immunofluorescence for FN (Fig. 2C) and collagen I (Fig. 2D) on MTM cells treated with vehicle (0.1% ethanol) or DEX (100 nM). Western blot analysis revealed decreased expression of FN and myocilin in GR<sup>dim</sup> MTM cells compared to WT MTM cells upon DEX treatment. Consistent with the Western blot analysis, immunostaining showed decreased production of FN and collagen I upon DEX treatment in GR<sup>dim</sup> MTM cells compared to WT MTM cells (Figs. 2C, 2D). This suggests that biochemical changes occurring in WT MTM cells in response to DEX treatment requires active GR TA. However, in GR<sup>dim</sup> mutants this function is impaired resulting in reduced or no effect of DEX in GR<sup>dim</sup> MTM cells.

### DEX-Induced CLAN Formation in GR<sup>dim</sup> MTM Cells

GCs reorganize the actin cytoskeleton in confluent TM cells by forming CLANs,<sup>30,32,78,79</sup> which are three-dimensional, geodesic dome-like structures and/or “tangles” of actin filaments. These morphologic changes increase TM stiffness and impair TM functions such as phagocytosis,<sup>34</sup> contractility, and proliferation,<sup>33</sup> adversely affecting the aqueous outflow pathway. To assess whether treatment with DEX will also induce CLAN formation in GR<sup>dim</sup> MTM cells, we compared CLAN formation with WT MTM cells (Fig. 3). After 1 week of DEX treatment, the percentage of CPCs increased significantly by 5.7-fold in WT MTM cells compared to a modest 1.8-fold increase in GR<sup>dim</sup> MTM cells. The percentage of CPCs was significantly higher in DEX-treated WT MTM cells than in DEX-treated GR<sup>dim</sup>, vehicle-treated (0.1% ethanol) control WT, and GR<sup>dim</sup> MTM cells (Fig. 3B). The absolute increase in percentage of CPCs in DEX-treated WT MTM cells ( $n = 3$ , experimental triplicates) was  $38.49\% \pm 1.9\%$  CPCs compared to  $6.75\% \pm 0.7\%$  CPCs in ethanol-treated ( $n = 2$ , experimental duplicates) WT MTM cells. Reduced CLAN formation was observed in GR<sup>dim</sup> MTM cells. The absolute increase in percentage of CPCs in DEX-treated GR<sup>dim</sup> MTM cells ( $n = 3$ , experimental triplicates) was  $15.53\% \pm 1.12\%$  CPCs compared to  $8.68\% \pm$

$0.9\%$  CPCs in ethanol-treated ( $n = 2$ , experimental duplicates) GR<sup>dim</sup> MTM cells (mean  $\pm$  standard error of the mean [SEM]). This suggests that the DEX-induced CLAN formation observed in the WT MTM cells required TA, and therefore GR<sup>dim</sup> MTM cells were significantly inhibited in generating DEX-induced CLANs.

### Effect of DEX-Ac Treatment on IOP in WT and GR<sup>dim</sup> Mice

We have previously shown that weekly periocular CF injections of a DEX-Ac suspension to both eyes of mice causes DEX-induced OHT with sustained and significantly elevated IOP in C57BL/6 mice.<sup>66,67</sup> DEX-Ac elevates IOP within 1 week of treatment as compared to vehicle-treated mice, and IOP elevation is sustained throughout the weeks of treatment. Since it has not yet been determined whether DEX leads to IOP elevation in GR<sup>dim</sup> mice, we injected DEX-Ac and compared IOP elevation in both WT and GR<sup>dim</sup> mice. The baseline IOPs for both WT and GR<sup>dim</sup> mice were the same, and the DEX-Ac-induced IOP elevation was rapid in WT mice compared to vehicle-treated mice starting from 1 week of treatment (Fig. 4A). However, DEX-Ac treatment did not elevate IOP in GR<sup>dim</sup> mice at any time point, and IOPs remained at baseline throughout the study (i.e., after 5 weeks of DEX-Ac treatment) even though these mice continued to receive weekly DEX-Ac treatment (Fig. 4B). In WT mice, the absolute increase in IOP in DEX-Ac-treated ( $n = 15$ ) versus vehicle-treated ( $n = 12$ ) mice averaged  $7.48 \pm 0.7$  mm Hg at day 7;  $9.76 \pm 0.8$  mm Hg at day 14;  $9.1 \pm 0.8$  mm Hg at day 21;  $10.67 \pm 1$  mm Hg at day 35; and  $10.27 \pm 0.9$  mm Hg at day 39 (mean  $\pm$  SEM;  $P < 0.0001$ ). However, in GR<sup>dim</sup> mice, the absolute increase in IOP in DEX-Ac-treated ( $n = 12$ ) versus vehicle-treated ( $n = 8$ ) mice was not significant and averaged  $1.12 \pm 0.9$  mm Hg at day 7;  $1.73 \pm 1.2$  mm Hg at day 14;  $0.45 \pm 0.8$  mm Hg at day 22;  $1.49 \pm 1$  mm Hg at day 29; and  $2.2 \pm 1.5$  mm Hg at day 36 (mean  $\pm$  SEM). These results suggest that DEX-Ac-induced IOP elevation requires fully functional GR TA, which was impaired in GR<sup>dim</sup> mice.

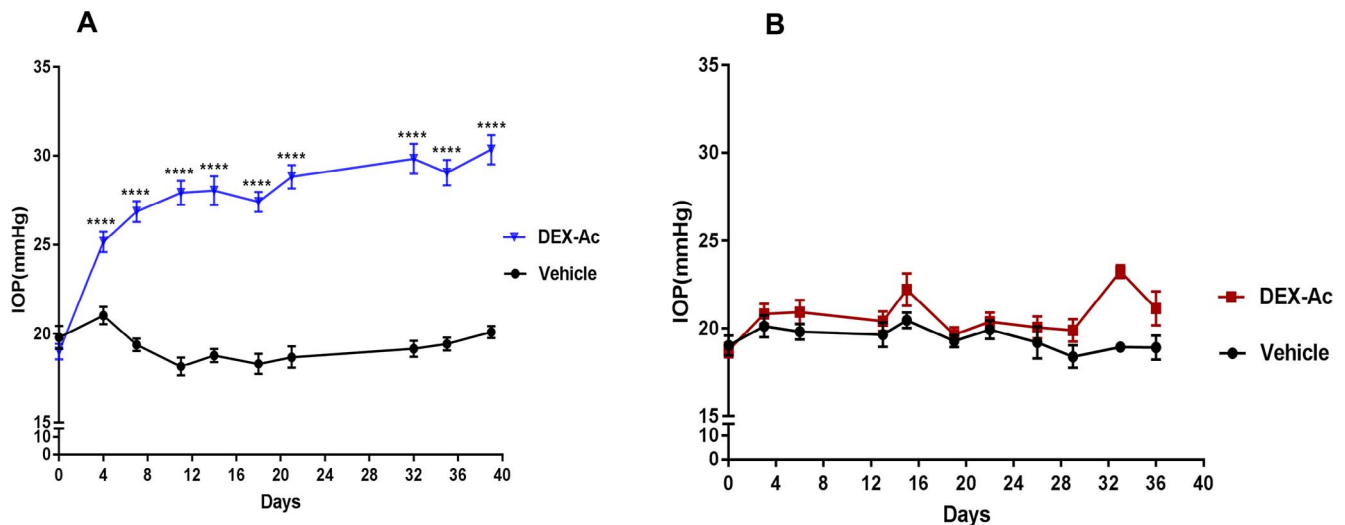


**FIGURE 4.** Inhibition of DEX-Ac-induced OHT in GR<sup>dim</sup> mice. **(A)** In WT mice, weekly periocular CF injections of DEX-Ac in both eyes significantly elevated IOP. Nighttime IOP measurements of DEX-Ac-treated ( $n = 15$ ) versus vehicle-treated ( $n = 12$ ) mice show significant IOP elevation from 4 to 39 days;  $****P < 0.0001$ . **(B)** In GR<sup>dim</sup> mice, weekly periocular CF injections of DEX-Ac in both eyes did not elevate IOP. Nighttime IOP measurements of DEX-Ac-treated ( $n = 12$ ) versus vehicle-treated ( $n = 8$ ) GR<sup>dim</sup> mice show no effect of IOP elevation from 4 to 36 days. Unpaired Student's *t*-test. Data are presented as mean  $\pm$  SEM.

### Effect of DEX-Ac Treatment on Conventional Outflow Facility in WT and GR<sup>dim</sup> Mice

Conventional outflow facility (C) was measured in live GR<sup>dim</sup> and WT mice after 5 weeks of DEX-Ac treatment. C was calculated according to the modified Goldman equation:  $IOP = [(F_{in} - F_u)/C] + P_e$ . In this equation,  $F_{in}$  represents aqueous humor production rate ( $\mu\text{L}/\text{min}$ ), C represents trabecular outflow facility ( $\mu\text{L}/\text{min}/\text{mm Hg}$ ),  $F_u$  represents uveoscleral outflow rate ( $\mu\text{L}/\text{min}$ ), and  $P_e$  represents episcleral venous pressure (mm Hg). We have previously shown that DEX-Ac treatment significantly reduces C in mice compared to vehicle-treated mice.<sup>66,67</sup> Similar results were observed in WT mice, and in our current study C was significantly reduced in DEX-Ac-treated mice compared to vehicle-treated mice (Fig. 5A). However, in GR<sup>dim</sup> mice, C remained unaffected in DEX-Ac-treated mice compared to vehicle-treated mice (Fig. 5B). In WT mice, C was  $10.12 \pm 0.9$  nL/min/mm Hg in DEX-Ac-treated mice ( $n = 8$ ) compared to  $22.80 \pm 3.2$  nL/min/mm Hg in vehicle-treated mice ( $P = 0.0007$ ;  $n = 5$ ). In contrast, C remained unchanged in GR<sup>dim</sup> mice and C was  $18.70 \pm 2.5$  nL/min/mm Hg in DEX-Ac-treated mice ( $n = 8$ ) compared  $18.00 \pm 2.7$  nL/min/mm Hg in vehicle-treated mice ( $n = 7$ ). No change in outflow facility corresponded well with the no change in IOP in GR<sup>dim</sup> mice upon DEX-Ac treatment. These results further confirm that DEX-Ac-induced reduction in outflow facility requires fully functional GR TA, which was impaired in GR<sup>dim</sup> mice.

### Immunohistologic Changes in the TM of WT and GR<sup>dim</sup> Mice After DEX-Ac Treatment

DEX treatment leads to many biochemical changes in the TM, including increased production of FN,<sup>36</sup> collagens,<sup>38</sup> and actin.<sup>30</sup> We have previously shown that these biochemical changes occur in our mouse model of DEX-Ac-induced OHT upon DEX-Ac treatment.<sup>66,67</sup> To assess whether treatment with DEX-Ac will also induce these biochemical changes in GR<sup>dim</sup> mice, we performed immunohistochemical analysis for FN, collagen I, and  $\alpha$ -SMA in anterior segment tissues from 5-week DEX-Ac-treated and vehicle-treated mice (Fig. 6). We also

compared them with WT DEX-Ac-treated and vehicle-treated mice. In WT mice, immunohistochemical analysis revealed increased FN, collagen I, and  $\alpha$ -SMA expression in the TM of DEX-Ac-treated mice compared to vehicle-treated mice (DEX-Ac,  $n = 6$ ; vehicle,  $n = 4$ ) (Figs. 6A, 6B). However, in GR<sup>dim</sup> mice, the expression of FN, collagen I, and  $\alpha$ -SMA remained unchanged in the TM of DEX-Ac-treated mice compared to vehicle-treated mice (DEX-Ac,  $n = 4$ ; vehicle,  $n = 2$ ) (Figs. 6C, 6D). These results are consistent with in vitro biochemical changes observed in MTM cells, suggesting that these biochemical changes occurring in the TM in response to DEX treatment require active GR TA. However, in GR<sup>dim</sup> mutants this function is impaired, resulting in reduced or no effect of DEX in the TM of GR<sup>dim</sup> mice.

### DISCUSSION

Higher GC doses and prolonged GC therapy cause a plethora of deleterious side effects including effects on eyes. Certain patients receiving prolonged GC therapy develop GC-OHT with open gonioscopic angles and increased resistance in the TM outflow pathway, similar to that seen in POAG. Currently, clinical management of GC-OHT in patients requires monitoring and lowering IOP with glaucoma drugs and/or surgery.<sup>21,22</sup> This elevated IOP, if left untreated, can lead to progressive optic nerve damage, optic disc cupping, and glaucomatous visual field defects. However, the molecular mechanisms responsible for GC-OHT are not entirely clear. The main physiological and pharmacologic actions of GCs are through the GR, a ligand-activated transcription factor. Biological changes after binding of GCs to the GR are mediated via TA or TR. It is assumed that the undesirable side effects of GC therapy require DNA-binding-mediated TA of GR, while the anti-inflammatory activities are due to TR in absence of GR DNA binding.<sup>47-49</sup> However, we did not know which of these GR mechanisms regulates GC-OHT, so we need better understanding of molecular mechanisms of GC action and GR signaling in the pathophysiology of GC-OHT in order to design GR agonists with a better benefit-risk ratio and more effective and safer treatment for patients. In our study, we used GR<sup>dim</sup> mice, which allowed us to determine which of these GR

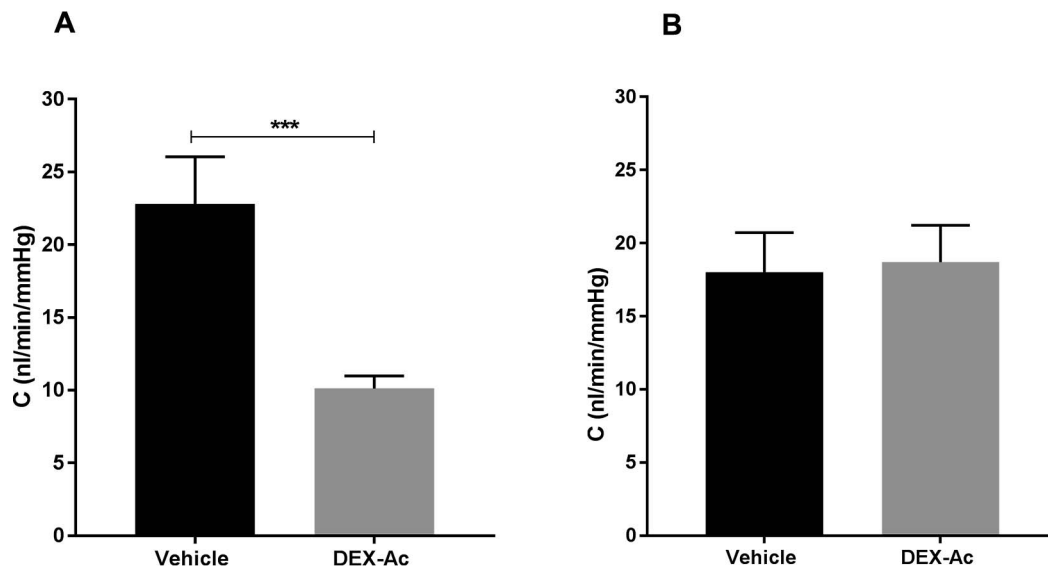


**FIGURE 5.** Comparison of conventional outflow facility (C) between DEX-Ac-treated and vehicle-treated WT and GR<sup>dim</sup> mice. (A) In WT mice, after 5 weeks of DEX-Ac treatment, C was significantly reduced in DEX-Ac-treated ( $n = 8$ ) mice compared to vehicle-treated ( $n = 5$ ) mice;  $P = 0.0007$ . (B) In GR<sup>dim</sup> mice, C remained unaffected in DEX-Ac-treated ( $n = 8$ ) mice compared to vehicle-treated ( $n = 7$ ) mice. Unpaired Student's  $t$ -test. Data are presented as mean  $\pm$  SEM.

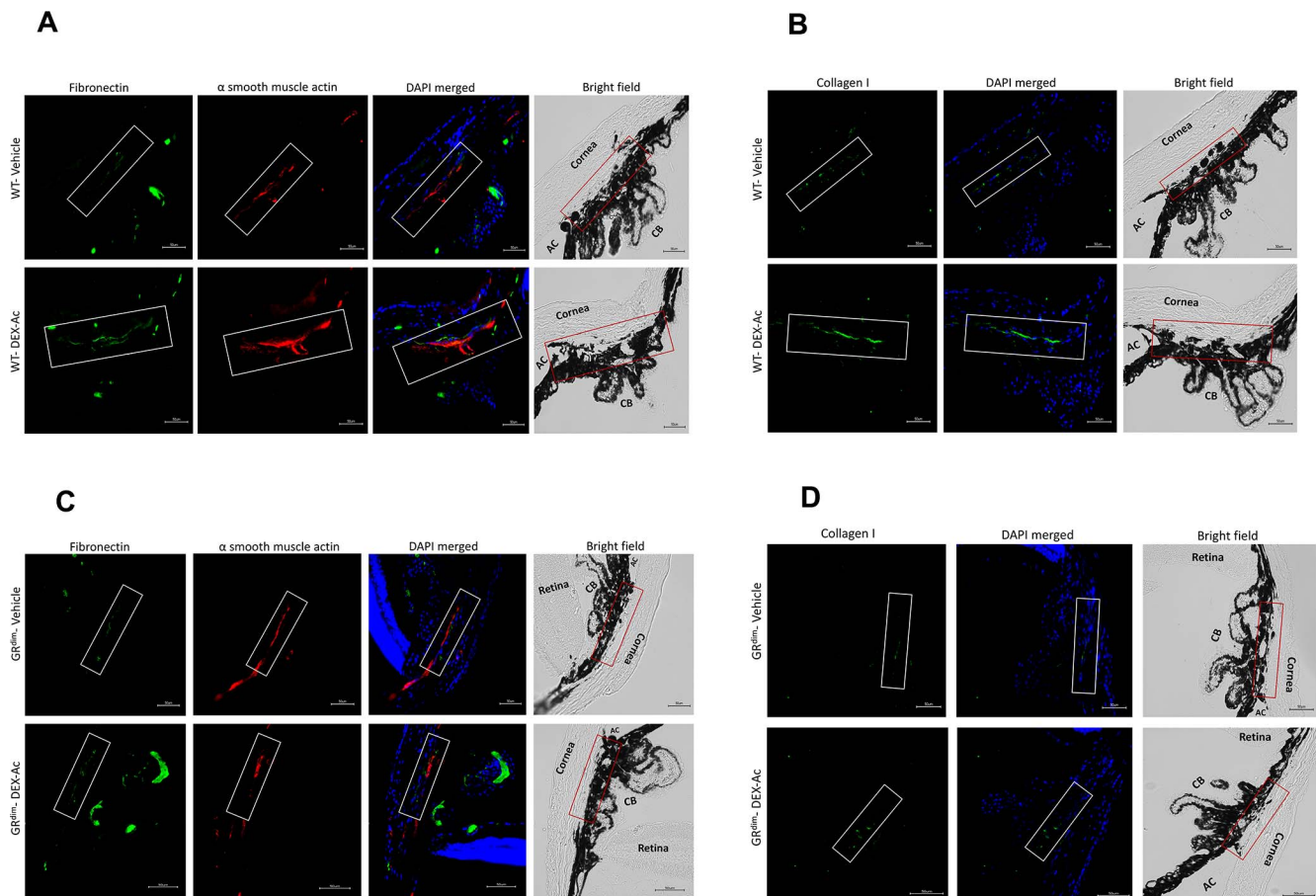


**FIGURE 6.** DEX-Ac treatment does not alter expression of fibronectin, collagen I, and  $\alpha$ -smooth muscle actin in the TM of GR<sup>dim</sup> mouse eyes. (A, B) Immunohistochemical analysis showing increased fibronectin (green) and  $\alpha$ -SMA (red) (A) as well as collagen I (green) (B) expression in the TM of DEX-Ac-treated mice compared to vehicle-treated WT mice (DEX-Ac,  $n = 6$ ; vehicle,  $n = 4$ ). (C, D) The expression of these proteins remains unchanged in the TM of DEX-Ac-treated GR<sup>dim</sup> mice compared to vehicle-treated GR<sup>dim</sup> mice (DEX-Ac,  $n = 4$ ; vehicle,  $n = 2$ ). DAPI staining (blue) counterstains cell nuclei. Bright field image showing structural orientation of TM with respect to other ocular structures. White and red rectangular box shows TM. Scale bar: 50  $\mu$ m.

mechanisms is responsible for GC-OHT. We showed that in GR<sup>dim</sup> mice there is reduced or no effects of GCs on MTM cells in vitro and GC-OHT in mouse eyes in vivo. There were no measured biochemical and morphologic changes observed in GR<sup>dim</sup> MTM cells upon GC treatment, as shown by no DEX-induced expression of FN, myocilin, and collagen I, and a very modest induction in GC-induced CLAN formation. Furthermore, GR<sup>dim</sup> mice did not develop GC-OHT or decreased conventional aqueous humor outflow facility upon DEX-Ac treatment. GR<sup>dim</sup> mice did not exhibit immunohistologic changes observed in the TM of GC-OHT eyes, including no apparent changes in the expression of FN, collagen type I, and  $\alpha$ -SMA in the TM region. These results suggest that GC-induced changes occurring in TM (including development of GC-OHT) require active GR TA. Therefore, these functions in GR<sup>dim</sup> mutants are impaired, resulting in reduced or no measured effects of GCs in the TM of GR<sup>dim</sup> mice.

We did not use full GR-/GR- knockout mice to study GR mechanisms regulating GC-OHT because they develop anomalies and die shortly after birth, demonstrating that both TA and TR functions of GR are essential for survival.<sup>80</sup> In contrast, GR<sup>dim</sup> mice remain viable and appear normal after birth.<sup>59</sup> GR<sup>dim</sup> mice have become an important research tool to dissect different GR functions because the point mutation A458T in the GR-DBD impairs GR dimerization. Therefore, altering the DNA-binding domain separates TA from TR activities because TA requires DNA binding of receptor homodimers to specific GREs to activate transcription of genes.<sup>81</sup> Although Presman and others<sup>82</sup> have questioned the exact molecular characteristics of the GR<sup>dim</sup> mutation,<sup>83,84</sup> this mouse strain has become an important tool to study the mode of GC actions in different diseases. Presman and colleagues<sup>82</sup> have used eGFP-tagged GRs and a new “number and brightness” microscopy technique to show that A458T mutation is not sufficient to prevent homodimerization. However, Beck et al.<sup>62</sup> mention various concerns when interpreting results from GR mutant-based experiments. They suggest that in cell lines expressing varying levels (low to high) of endogenous GR, transient transfection with GR constructs to overexpress excessive and nonphysiological levels of GR could possibly cause artefactual results. This could be one of the reasons Presman and colleagues<sup>82</sup> have not seen sufficient effects of the A458T mutation. In addition, Beck and colleagues<sup>62</sup> also mention that to study a GR mutant, it is best to express the GR mutant of interest into a genome placed under the control of its endogenous promoter in an in vivo system. Thus, we have used GR<sup>dim</sup> transgenic mice to study the role of GR functions in regulating GC-OHT.

Interestingly, many of the immunosuppressive and anti-inflammatory properties of GCs are mediated by GR-TR mechanisms in absence of DNA binding, while GR-TA largely accounts for GC treatment side effects.<sup>85,86</sup> Considerable efforts are being made to improve benefit-risk ratio of GCs by designing compounds classified as SEGRAs or SEGRMs, which promote TR but do not mediate TA.<sup>47</sup> However, some side effects such as GC-induced osteoporosis are mediated by both TA and TR, so SEGRAs do not eliminate all undesirable GC side effects. In addition, some of the GC-mediated immunosuppressive activities also involve both GR-mediated TA and TR pathways.<sup>47</sup> Our studies using GR<sup>dim</sup> mice will serve as a genetic model for a novel class of potential selective GR modulators<sup>49,87</sup> and also will tease out mechanisms by which GR mediates its desirable anti-inflammatory/immunomodulatory effects on the eye and undesirable effects on the TM. Several studies evaluating effects of SEGRAs on cultured monkey<sup>57</sup> and human TM cells<sup>58</sup> have reported variable responses to gene expression (i.e., myocilin and FN) as compared to conventional GCs. It appeared that SEGRAs did not induce myocilin and FN expression as compared to GCs. These studies suggest that

reduced GR-TA may limit effects on the conventional outflow pathway and on IOP. Our studies with GR<sup>dim</sup> mice (which have active TR and impaired TA) showed that blocking GR-TA inhibits many GC effects on the TM in vitro and GC-OHT in vivo as compared to WT mice (which have both TA and TR mechanisms). WT mice developed GC-OHT similar to what we have previously described.<sup>66,67</sup>

GCs have a wide variety of effects on TM cells and tissues,<sup>23,28</sup> only some of which were tested in our current study. It also will be important to use GR<sup>dim</sup> mice and MTM cells to determine whether GR TA is responsible for altered growth factor responsiveness,<sup>23</sup> alterations in cell junctions,<sup>88,89</sup> inhibition of the Wnt canonical pathway,<sup>40</sup> induction of TGF $\beta$ 2,<sup>90</sup> enlarged cellular and nuclear size,<sup>33</sup> changes in the glycosaminoglycan profile,<sup>91</sup> activation of endoplasmic reticulum (ER) stress,<sup>92</sup> and inhibition of migration and proliferation,<sup>33</sup> any or all of which may be responsible for GC-OHT.

In summary, our current work provides the first evidence of the role of GR TA in regulating GC-mediated gene expression in the TM and GC-OHT in mice. Upon GC treatment, GR<sup>dim</sup> mice did not develop elevated IOP, reduced conventional aqueous humor outflow facility, or GC-mediated biochemical and morphologic changes in the TM.

### Acknowledgments

The authors thank Sandra Maansson and Sherri Harris for technical assistance.

Supported by National Eye Institute (NEI) Grant EY016242 (AFC).

Disclosure: **G.C. Patel**, None; **J.C. Millar**, None; **A.F. Clark**, Goodmans LLP (C)

### References

1. Ramamoorthy S, Cidlowski JA. Corticosteroids: mechanisms of action in health and disease. *Rheum Dis Clin North Am*. 2016;42:15-31.
2. Fini ME, Schwartz SG, Gao X, et al. Steroid-induced ocular hypertension/glaucoma: focus on pharmacogenomics and implications for precision medicine. *Prog Retin Eye Res*. 2017;56:58-83.
3. Rhen T, Cidlowski JA. Antiinflammatory action of glucocorticoids: new mechanisms for old drugs. *N Engl J Med*. 2005; 353:1711-1723.
4. Overman RA, Yeh JY, Deal CL. Prevalence of oral glucocorticoid usage in the United States: a general population perspective. *Arthritis Care Res (Hoboken)*. 2013;65:294-298.
5. Fardet L, Petersen I, Nazareth I. Prevalence of long-term oral glucocorticoid prescriptions in the UK over the past 20 years. *Rheumatology (Oxford)*. 2011;50:1982-1990.
6. Jabs DA, Rosenbaum JT, Foster CS, et al. Guidelines for the use of immunosuppressive drugs in patients with ocular inflammatory disorders: recommendations of an expert panel. *Am J Ophthalmol*. 2000;130:492-513.
7. Hunter RS, Lobo AM. Dexamethasone intravitreal implant for the treatment of noninfectious uveitis. *Clin Ophthalmol*. 2011;5:1613-1621.
8. Kempen JH, Altaweel MM, Holbrook JT, et al.; Multicenter Uveitis Steroid Treatment Trial Research Group. The multicenter uveitis steroid treatment trial: rationale, design, and baseline characteristics. *Am J Ophthalmol*. 2010;149:550-561.e10.
9. Haller JA, Bandello F, Belfort R Jr, et al. Dexamethasone intravitreal implant in patients with macular edema related to branch or central retinal vein occlusion twelve-month study results. *Ophthalmology*. 2011;118:2453-2460.

10. Elman MJ, Aiello LP, Beck RW, et al.; Diabetic Retinopathy Clinical Research Network. Randomized trial evaluating ranibizumab plus prompt or deferred laser or triamcinolone plus prompt laser for diabetic macular edema. *Ophthalmology*. 2010;117:1064-1077.e35.
11. Schwartz SG, Flynn HW Jr, Beer P. Intravitreal triamcinolone acetate use in diabetic macular edema: illustrative cases. *Ophthalmic Surg Lasers Imaging*. 2010;42:E1-E6.
12. Price FW Jr, Price DA, Ngakeng V, Price MO. Survey of steroid usage patterns during and after low-risk penetrating keratoplasty. *Cornea*. 2009;28:865-870.
13. Vajaranant TS, Price MO, Price FW, Gao W, Wilensky JT, Edward DP. Visual acuity and intraocular pressure after Descemet's stripping endothelial keratoplasty in eyes with and without preexisting glaucoma. *Ophthalmology*. 2009;116:1644-1650.
14. Ray S, Mehra KS, Misra S, Singh R. Plasma cortisol in glaucoma. *Ann Ophthalmol*. 1977;9:1151-1154.
15. Rozsival P, Hampf R, Obenberger J, Starka L, Rehak S. Aqueous humour and plasma cortisol levels in glaucoma and cataract patients. *Curr Eye Res*. 1981;1:391-396.
16. Meredig WE, Jentzen F, Hartmann F. Systemic side effects of topically applied corticosteroid medication (author's transl) [in German]. *Klin Monbl Augenheilkd*; 1980;176:907-910.
17. Schwartz B, Seddon JM. Increased plasma cortisol levels in ocular hypertension. *Arch Ophthalmol*. 1981;99:1791-1794.
18. McCarty GR, Schwartz B. Increased plasma noncortisol glucocorticoid activity in open-angle glaucoma. *Invest Ophthalmol Vis Sci*. 1991;32:1600-1608.
19. Southren AL, Gordon GG, Munnangi PR, et al. Altered cortisol metabolism in cells cultured from trabecular meshwork specimens obtained from patients with primary open-angle glaucoma. 1983;24:1413-1417.
20. Weinstein BI, Munnangi P, Gordon GG, Southren AL. Defects in cortisol-metabolizing enzymes in primary open-angle glaucoma. *Invest Ophthalmol Vis Sci*. 1985;26:890-893.
21. Kersey JP, Broadway DC. Corticosteroid-induced glaucoma: a review of the literature. *Eye (Lond)*. 2006;20:407-416.
22. Jones R III, Rhee DJ. Corticosteroid-induced ocular hypertension and glaucoma: a brief review and update of the literature. *Curr Opin Ophthalmol*. 2006;17:163-167.
23. Clark AF, Wordinger RJ. The role of steroids in outflow resistance. *Exp Eye Res*. 2009;88:752-759.
24. Armaly MF. Statistical attributes of the steroid hypertensive response in the clinically normal eye, I: the demonstration of three levels of response. *Invest Ophthalmol*. 1965;4:187-197.
25. Armaly MF, Becker B. Intraocular pressure response to topical corticosteroids. *Fed Proc*. 1965;24:1274-1278.
26. Grant WM. Experimental aqueous perfusion in enucleated human eyes. *Arch Ophthalmol*. 1963;69:783-801.
27. Stamer WD, Clark AF. The many faces of the trabecular meshwork cell. *Exp Eye Res*. 2017;158:112-123.
28. Wordinger RJ, Clark AF. Effects of glucocorticoids on the trabecular meshwork: towards a better understanding of glaucoma. *Prog Retin Eye Res*. 1999;18:629-667.
29. Bermudez JY, Montecchi-Palmer M, Mao W, Clark AF. Cross-linked actin networks (CLANs) in glaucoma. *Exp Eye Res*. 2017;159:16-22.
30. Clark AF, Brotchie D, Read AT, et al. Dexamethasone alters F-actin architecture and promotes cross-linked actin network formation in human trabecular meshwork tissue. *Cell Motil Cytoskeleton*. 2005;60:83-95.
31. Hoare MJ, Grierson I, Brotchie D, Pollock N, Cracknell K, Clark AF. Cross-linked actin networks (CLANs) in the trabecular meshwork of the normal and glaucomatous human eye in situ. *Invest Ophthalmol Vis Sci*. 2009;50:1255-1263.
32. O'Reilly S, Pollock N, Currie L, Paraoan L, Clark AF, Grierson I. Inducers of cross-linked actin networks in trabecular meshwork cells. *Invest Ophthalmol Vis Sci*. 2011;52:7316-7324.
33. Clark AF, Wilson K, McCartney MD, Miggans ST, Kunkle M, Howe W. Glucocorticoid-induced formation of cross-linked actin networks in cultured human trabecular meshwork cells. *Invest Ophthalmol Vis Sci*. 1994;35:281-294.
34. Zhang X, Ognibene CM, Clark AF, Yorio T. Dexamethasone inhibition of trabecular meshwork cell phagocytosis and its modulation by glucocorticoid receptor beta. *Exp Eye Res*. 2007;84:275-284.
35. Johnson DH, Bradley JMB, Acott TS. The effect of dexamethasone on glycosaminoglycans of human trabecular meshwork in perfusion organ culture. *Invest Ophthalmol Vis Sci*. 1990;31:2568-2571.
36. Steely HT, Browder SL, Julian MB, Miggans ST, Wilson KL, Clark AF. The effects of dexamethasone on fibronectin expression in cultured human trabecular meshwork cells. *Invest Ophthalmol Vis Sci*. 1992;33:2242-2250.
37. Dickerson JE Jr, Steely HT Jr, English-Wright SL, Clark AF. The effect of dexamethasone on integrin and laminin expression in cultured human trabecular meshwork cells. *Exp Eye Res*. 1998;66:731-738.
38. Zhou L, Li Y, Yue BY. Glucocorticoid effects on extracellular matrix proteins and integrins in bovine trabecular meshwork cells in relation to glaucoma. *Int J Mol Med*. 1998;1:339-346.
39. Yun AJ, Murphy CG, Polansky JR, Newsome DA, Alvarado JA. Proteins secreted by human trabecular cells: glucocorticoid and other effects. *Invest Ophthalmol Vis Sci*. 1989;30:2012-2022.
40. Raghunathan VK, Morgan JT, Park SA, et al. Dexamethasone stiffens trabecular meshwork, trabecular meshwork cells, and matrix. *Invest Ophthalmol Vis Sci*. 2015;56:4447-4459.
41. Wang K, Li G, Read AT, Navarro I, et al. The relationship between outflow resistance and trabecular meshwork stiffness in mice. *Sci Rep*. 2018;8:5848.
42. Cruz-Topete D, Cidlowski JA. One hormone, two actions: anti- and pro-inflammatory effects of glucocorticoids. *Neuroimmunomodulation*. 2015;22:20-32.
43. Hollenberg SM, Weinberger C, Ong ES, et al. Primary structure and expression of a functional human glucocorticoid receptor cDNA. *Nature*. 1985;318:635-641.
44. Encio IJ, Detera-Wadleigh SD. The genomic structure of the human glucocorticoid receptor. *J Biol Chem*. 1991;266:7182-7188.
45. Grad I, Picard D. The glucocorticoid responses are shaped by molecular chaperones. *Mol Cell Endocrinol*. 2007;275:2-12.
46. Pratt WB, Toft DO. Steroid receptor interactions with heat shock protein and immunophilin chaperones. *Endocr Rev*. 1997;18:306-360.
47. Sundahl N, Bridelance J, Libert C, De Bosscher K, Beck IM. Selective glucocorticoid receptor modulation: new directions with non-steroidal scaffolds. *Pharmacol Ther*. 2015;152:28-41.
48. Cain DW, Cidlowski JA. Specificity and sensitivity of glucocorticoid signaling in health and disease. *Best Pract Res Clin Endocrinol Metab*. 2015;29:545-556.
49. Kleiman A, Tuckermann JP. Glucocorticoid receptor action in beneficial and side effects of steroid therapy: lessons from conditional knockout mice. *Mol Cell Endocrinol*. 2007;275:98-108.
50. Reichardt SD, Weinlage T, Rotte A, et al. Glucocorticoids induce gastroparesis in mice through depletion of l-arginine. *Endocrinology*. 2014;155:3899-3908.
51. Quinn M, Ramamoorthy S, Cidlowski JA. Sexually dimorphic actions of glucocorticoids: beyond chromosomes and sex hormones. *Ann N Y Acad Sci*. 2014;1317:1-6.

52. De Bosscher K, Haegeman G, Elewaut D. Targeting inflammation using selective glucocorticoid receptor modulators. *Curr Opin Pharmacol*. 2010;10:497-504.
53. De Bosscher K, Vanden Berghe W, Beck IM, et al. A fully dissociated compound of plant origin for inflammatory gene repression. *Proc Natl Acad Sci U S A*. 2005;102:15827-15832.
54. Robertson S, Allie-Reid F, Vanden Berghe W, et al. Abrogation of glucocorticoid receptor dimerization correlates with dissociated glucocorticoid behavior of compound a. *J Biol Chem*. 2010;285:8061-8075.
55. Lesovaya E, Yemelyanov A, Swart AC, Swart P, Haegeman G, Budunova I. Discovery of Compound A: a selective activator of the glucocorticoid receptor with anti-inflammatory and anti-cancer activity. *Oncotarget*. 2015;6:30730-30744.
56. Jaroch S, Berger M, Huwe C, et al. Discovery of quinolines as selective glucocorticoid receptor agonists. *Bioorg Med Chem Lett*. 2010;20:5835-5838.
57. Pfeffer BA, DeWitt CA, Salvador-Silva M, Cavet ME, Lopez FJ, Ward KW. Reduced myocilin expression in cultured monkey trabecular meshwork cells induced by a selective glucocorticoid receptor agonist: comparison with steroids. *Invest Ophthalmol Vis Sci*. 2010;51:437-446.
58. Stamer WD, Hoffman EA, Kurali E, Krauss AH. Unique response profile of trabecular meshwork cells to the novel selective glucocorticoid receptor agonist, GW870086X. *Invest Ophthalmol Vis Sci*. 2013;54:2100-2107.
59. Reichardt HM, Kaestner KH, Tuckermann J, et al. DNA binding of the glucocorticoid receptor is not essential for survival. *Cell*. 1998;93:531-541.
60. Alroy I, Freedman LP. DNA binding analysis of glucocorticoid receptor specificity mutants. *Nucleic Acids Res*. 1992;20:1045-1052.
61. Schena M, Freedman LP, Yamamoto KR. Mutations in the glucocorticoid receptor zinc finger region that distinguish interdigitated DNA binding and transcriptional enhancement activities. *Genes Dev*. 1989;3:1590-1601.
62. Beck IM, De Bosscher K, Haegeman G. Glucocorticoid receptor mutants: man-made tools for functional research. *Trends Endocrinol Metab*. 2011;22:295-310.
63. Reichardt HM, Tuckermann JP, Göttlicher M, et al. Repression of inflammatory responses in the absence of DNA binding by the glucocorticoid receptor. *EMBO J*. 2001;20:7168-7173.
64. Frijters R, Fleuren W, Toonen EJ, et al. Prednisolone-induced differential gene expression in mouse liver carrying wild type or a dimerization-defective glucocorticoid receptor. *BMC Genomics*. 2010;11:359.
65. Tuckermann JP, Reichardt HM, Arribas R, Richter KH, Schütz G, Angel P. The DNA binding-independent function of the glucocorticoid receptor mediates repression of Ap-1-dependent genes in skin. 1999;147:1365-1370.
66. Patel GC, Phan TN, Maddineni P, et al. Dexamethasone-induced ocular hypertension in mice: effects of myocilin and route of administration. *Am J Pathol*. 2017;187:713-723.
67. Patel GC, Liu Y, Millar JC, Clark AF. Glucocorticoid receptor GRbeta regulates glucocorticoid-induced ocular hypertension in mice. *Sci Rep*. 2018;8:862.
68. Millar JC, Clark AF, Pang I-H. Assessment of aqueous humor dynamics in the mouse by a novel method of constant-flow infusion. *Invest Ophthalmol Vis Sci*. 2011;52:685-694.
69. Millar JC, Phan TN, Pang I-H, Clark AF. Strain and age effects on aqueous humor dynamics in the mouse aqueous humor dynamics by strain and age. *Invest Ophthalmol Vis Sci*. 2015;56:5764-5776.
70. Mao W, Liu Y, Wordinger RJ, Clark AF. A magnetic bead-based method for mouse trabecular meshwork cell isolation. *Invest Ophthalmol Vis Sci*. 2013;54:3600-3606.
71. Kasetti RB, Phan TN, Millar JC, Zode GS. Expression of mutant myocilin induces abnormal intracellular accumulation of selected extracellular matrix proteins in the trabecular meshwork. *Invest Ophthalmol Vis Sci*. 2016;57:6058-6069.
72. Montecchi-Palmer M, Bermudez JY, Webber HC, Patel GC, Clark AF, Mao W. TGFβ2 induces the formation of cross-linked actin networks (CLANs) in human trabecular meshwork cells through the Smad and non-Smad dependent pathways. *Invest Ophthalmol Vis Sci*. 2017;58:1288-1295.
73. Bill A. Editorial: the drainage of aqueous humor. *Invest Ophthalmol*. 1975;14:1-3.
74. Johnson DH, Richardson TM, Epstein DL. Trabecular meshwork recovery after phagocytic challenge. *Curr Eye Res*. 1989;8:1121-1130.
75. Buller C, Johnson DH, Tschumper RC. Human trabecular meshwork phagocytosis: observations in an organ culture system. *Invest Ophthalmol Vis Sci*. 1990;31:2156-2163.
76. Schlotzer-Schrehardt U, Naumann GO. Trabecular meshwork in pseudoexfoliation syndrome with and without open-angle glaucoma: a morphometric, ultrastructural study. *Invest Ophthalmol Vis Sci*. 1995;36:1750-1764.
77. Polansky JR, Fauss DJ, Chen P, et al. Cellular pharmacology and molecular biology of the trabecular meshwork inducible glucocorticoid response gene product. *Ophthalmologica*. 1997;211:126-139.
78. Mao W, Liu Y, Mody A, Montecchi-Palmer M, Wordinger RJ, Clark AF. Characterization of a spontaneously immortalized bovine trabecular meshwork cell line. *Exp Eye Res*. 2012;105:53-59.
79. Wade NC, Grierson I, O'Reilly S, et al. Cross-linked actin networks (CLANs) in bovine trabecular meshwork cells. *Exp Eye Res*. 2009;89:648-659.
80. Cole TJ, Blendy JA, Monaghan AP, et al. Targeted disruption of the glucocorticoid receptor gene blocks adrenergic chromaffin cell development and severely retards lung maturation. *Genes Dev*. 1995;9:1608-1621.
81. Heck S, Kullmann M, Gast A, et al. A distinct modulating domain in glucocorticoid receptor monomers in the repression of activity of the transcription factor AP-1. *EMBO J*. 1994;13:4087-4095.
82. Presman DM, Ogara ME, Stortz M, et al. Live cell imaging unveils multiple domain requirements for in vivo dimerization of the glucocorticoid receptor. *PLoS Biol*. 2014;12:e1001813.
83. Jewell CM, Scoltock AB, Hamel BL, Yudt MR, Cidlowski JA. Complex human glucocorticoid receptor dim mutations define glucocorticoid induced apoptotic resistance in bone cells. *Mol Endocrinol*. 2012;26:244-256.
84. Roohk DJ, Mascharak S, Khambatta C, Leung H, Hellerstein M, Harris C. Dexamethasone-mediated changes in adipose triacylglycerol metabolism are exaggerated, not diminished, in the absence of a functional GR dimerization domain. *Endocrinology*. 2013;154:1528-1539.
85. Kassel O, Herrlich P. Crosstalk between the glucocorticoid receptor and other transcription factors: molecular aspects. *Mol Cell Endocrinol*. 2007;275:13-29.
86. Karin M. New twists in gene regulation by glucocorticoid receptor: is DNA binding dispensable? *Cell*. 1998;93:487-490.
87. Schäcke H, Schottelius A, Döcke W-D, et al. Dissociation of transactivation from transrepression by a selective glucocorticoid receptor agonist leads to separation of therapeutic effects from side effects. *Proc Natl Acad Sci U S A*. 2004;101:227-232.
88. Faralli JA, Gagen D, Filla MS, Crotti TN, Peters DM. Dexamethasone increases alpha5beta3 integrin expression and affinity through a calcineurin/NFAT pathway. *Biochim Biophys Acta*. 2013;1833:3306-3313.
89. Underwood JL, Murphy CG, Chen J, et al. Glucocorticoids regulate transendothelial fluid flow resistance and formation

- of intercellular junctions. *Am J Physiol.* 1999;277:C330-C342.
90. Kasseti RB, Maddineni P, Patel P, Searby S, Sheffield VC, Zode GS. Transforming growth factor b2 (tGFb2) signaling plays a key role in glucocorticoid-induced ocular hypertension. *J Biol Chem.* 2018;293:9854-9868.
91. Johnson DH, Knepper PA. Microscale analysis of the glycosaminoglycans of human trabecular meshwork: a study in perfusion cultured eyes. *J Glaucoma.* 1994;3:58-69.
92. Zode GS, Sharma AB, Lin X, et al. Ocular-specific ER stress reduction rescues glaucoma in murine glucocorticoid-induced glaucoma. *J Clin Invest.* 2014;124:1956-1965.